

Supporting information for

Guiding Zn Uniform Deposition with Multifunctional additive for Highly Utilized Zn Anode

Xi Li,^{a,b} Zhenjie Chen,^b Pengchao Ruan,^c Xueting Hu,^c Xiaoming Yuan,^d Bingan Lu,^e Liping Qin^{a,}
and Jiang Zhou^{c,*}*

^a College of Biological and Chemical Engineering, Guangxi University of Science and Technology, Liuzhou 545006, Guangxi, China. E-mail: qinlp2005@126.com

^b Hunan Provincial Key Laboratory of Flexible Electronic Materials Genome Engineering, Changsha University of Science and Technology, Changsha 410004, Hunan, China

^c School of Materials Science and Engineering, Hunan Provincial Key Laboratory of Electronic Packaging and Advanced Functional Materials, Central South University, Changsha 410083, Hunan, China, E-mail: zhou_jiang@csu.edu.cn

^d Hunan Key Laboratory of Nanophotonics and Devices, School of Physics, Central South University, 932 South Lushan Road, Changsha 410083, Hunan, China

^e School of Physics and Electronics, Hunan University, Changsha 410082, Hunan, China

Corresponding author: E-mail: qinlp2005@126.com; zhou_jiang@csu.edu.cn

Experimental section

Materials: L-Leucine ($C_6H_{13}NO_2$, $\geq 99\%$), Ammonium metavanadate (NH_4VO_3 , 99.95%), Zinc sulfate ($ZnSO_4 \cdot 7H_2O$, 99%) and N-methyl pyrrolidone (NMP, $> 99\%$) were purchased from Shanghai Aladdin Biochemical Technology Co., Ltd. Ethanedioic acid dihydrate ($H_2C_2O_4 \cdot 2H_2O$, $\geq 99.8\%$) was purchased from Sinopharm Chemical Reagent Co., Ltd. Super P (battery grade) and polyvinylidene fluoride (PVDF, battery grade) were purchased from Soochow DoDoChem Technology Co., Ltd.

Electrolyte preparation: $ZnSO_4 \cdot 7H_2O$ was dissolved into deionized (DI) water to prepare the 2 M $ZnSO_4$ (ZS) electrolyte. Different concentrations (10, 20, 50, 100 mM) of L-Leucine (Leu) were added into the 2 M $ZnSO_4$ solutions (denoted as Leu10, Leu 20, Leu 50 and Leu100) to obtain the electrolytes for subsequent tests.

Preparation of $NH_4V_4O_{10}$ cathode materials: 2.106 g of NH_4VO_3 was dissolved in 90 mL of DI water and stirred at 80 °C until the solution became yellow. Then, 3.4038 g of $H_2C_2O_4 \cdot 2H_2O$ was added slowly and kept stirring to obtain a dark blue-green solution. The obtained solution was transferred to a 50 mL Teflon-lined autoclave and kept at 140 °C for 48 hours. The solid materials were collected and repeatedly washed with DI water and then dried at 80 °C overnight to obtain the $NH_4V_4O_{10}$ powers.

Material characterizations: X-ray diffraction (XRD) measurements were carried out on the Rigaku Mini Flex 600 diffractometer with Cu $K\alpha$ -radiation ($\lambda = 1.5418 \text{ \AA}$). The surface morphology of Zn anodes was characterized by an optical microscope (LW50LJT) and scanning electron microscope (SEM, MIRA3 TESCAN, 10 kV).

Electrochemical measurements: All CR2016-type coin cells using glass fiber separators were assembled in an open-air environment. Galvanostatic charge-discharge (GCD) cycling tests were conducted at room temperature on NEWARE battery tester (CT-4008T-5V50mA-164) and LAND battery tester (LAND CT2001, China). Cyclic voltammetry (CV), chronoamperometry (CA) and

electrochemical impedance spectroscopy (EIS) tests were performed on an electrochemical workstation (CHI660E, China). Linear sweep voltammetry (LSV) tests were performed at a scan rate of 5 mV s^{-1} in a three-electrode configuration, in which an Ag/AgCl electrode was used as the reference electrode. In the LSV tests, all the electrolytes were based on 1 M Na_2SO_4 solutions.

Density functional theory (DFT) calculations: The DFT was utilized to investigate the interactions of H_2O , Leu, and Zn^{2+} on different Zn crystal planes. The adsorption energies of them were calculated by the Vienna ab initio simulation package (VASP). The generalized gradient approximation (GGA) with the Perdew-Burke-Ernzerhof (PBE) function was used as the exchange-correlation function. Firstly, we generated k-point meshes using VASPKIT with a $3 \times 5 \times 1$ k-point mesh in the Monkhorst-Pack scheme, and the cutoff energy was set as 500 eV. Next, the convergence criteria of energy and force were set as 1×10^{-6} eV and 0.02 eV/atom, respectively. The Zn (002) surface had a 4×4 supercell in the *ab* dimension. The adsorption energies between the Zn slab and various particles were defined by the following equation:

$$E_{\text{aborb}} = E_{\text{tot}} - E_{\text{Zn-slab}} - E_{\text{molecules}}$$

where E_{aborb} , E_{tot} , $E_{\text{Zn-slab}}$ and $E_{\text{molecules}}$ represent the adsorption energy, total energy of the system, energy of the Zn slab and energy of the isolated adsorbed molecules, respectively.

Molecular dynamics (MD) simulations: Molecular dynamics (MD) simulations were conducted with GROMACS2020.3. The simulation system was constructed with PACKMOL by uniformly mixing H_2O , ZnSO_4 , and leu molecules with the number of 3000, 108 and 2, respectively. The SPC/E water model was employed for water. The force field parameters of SO_4^{2-} were from the literature¹ while the Zn^{2+} ions were taken from the Amber03 force field. The parameters of leu were created with Sobotop software². RESP atom charges calculated from Multiwfn³ were used to describe the electrostatic interactions. The short-range non-bonding interactions were calculated within a cutoff distance of 1.2 nm, and the particle mesh Ewald (PME) summation method was used to calculate electrostatic interactions. The energy minimization was first performed for all boxes by the steepest descent method. The equilibrium simulations were performed with an NPT ensemble at 298.2 K and 1 bar for 20 ns with an integration step of 2 fs. The last 10 ns was used for analysis.

The visualization of molecular structure and the radial distribution function (RDF) were obtained using VMD software⁴.

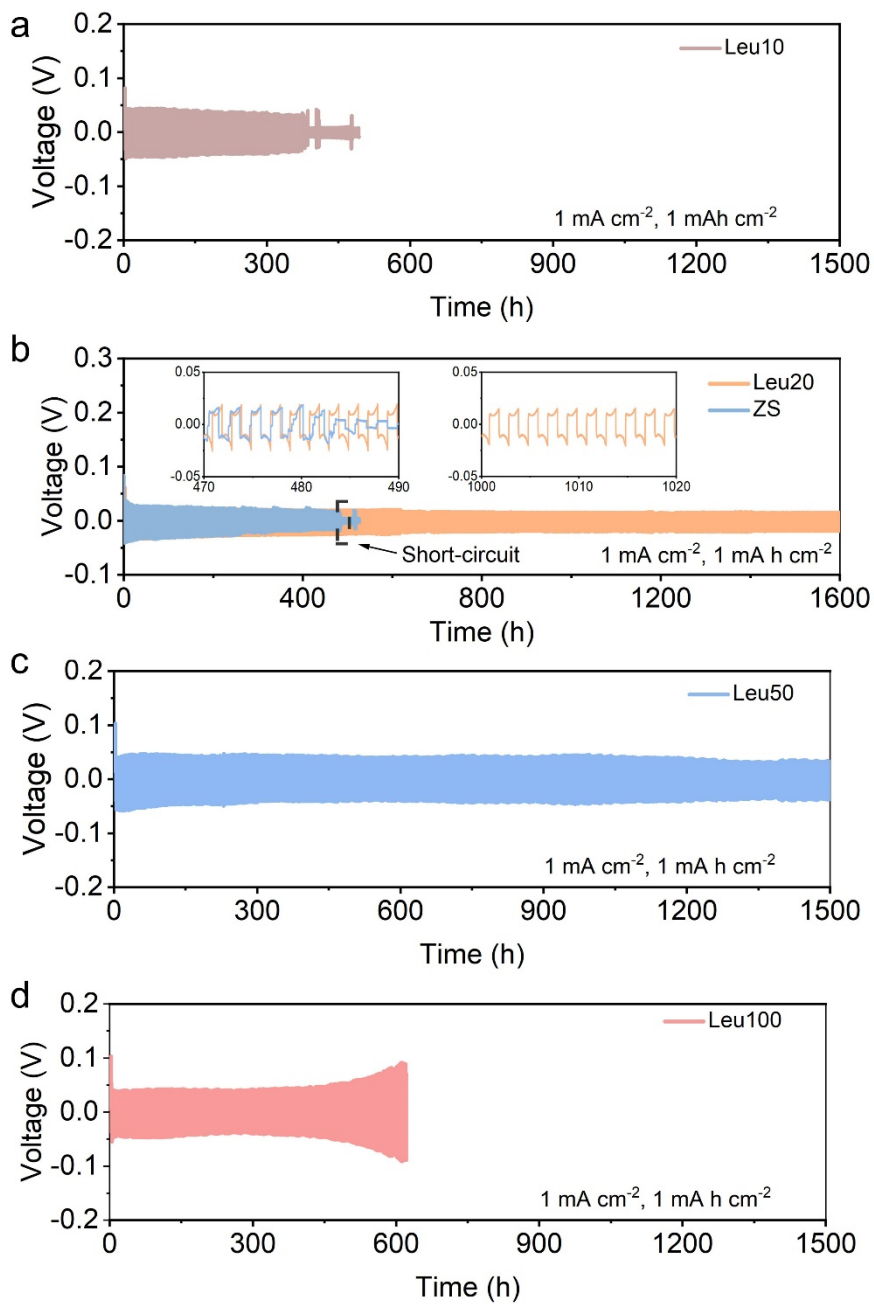


Fig. S1. Long-term cycling performance of Zn||Zn symmetric cells based on (a) Leu10, (b) Leu20, (c) Leu50 and (d) Leu100 electrolytes at 1 mA cm^{-2} , 1 mA h cm^{-2} .



Fig. S2. Optical image of Zn anode based on ZS electrolyte after cycling at 5 mA cm^{-2} , 5 mA h cm^{-2} .

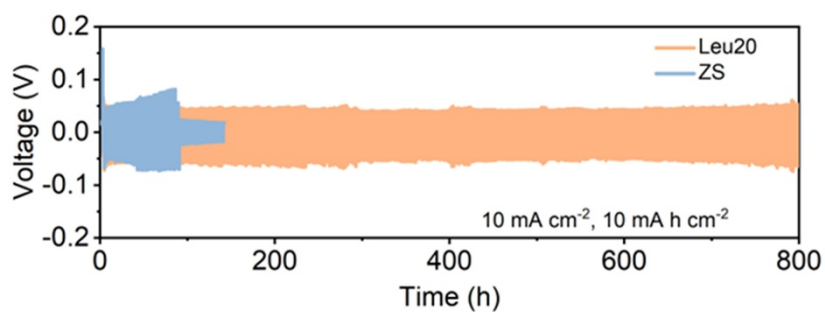


Fig. S3. Long-term cycling performance of Zn||Zn symmetric cells with Leu20 and ZS electrolytes at 10 mA cm^{-2} , 10 mA h cm^{-2} .

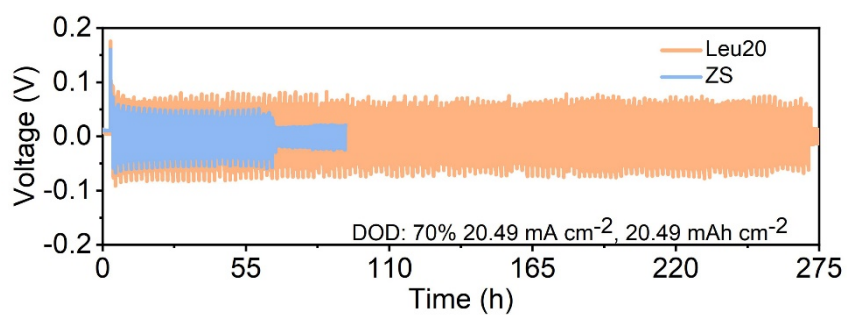


Fig. S4. Long-term cycling performance of Zn||Zn symmetric cells with Leu20 and ZS electrolytes at 20.49 mA cm^{-2} , $20.49 \text{ mA h cm}^{-2}$.

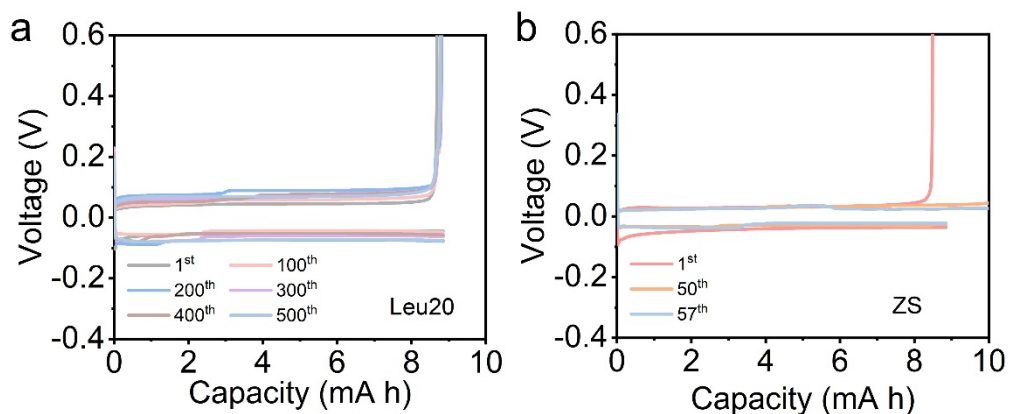


Fig. S5. Voltage profiles of Zn||Cu asymmetric cells based on (a) Leu20 and (b) ZS electrolytes at 5 mA cm⁻², 5 mA h cm⁻².

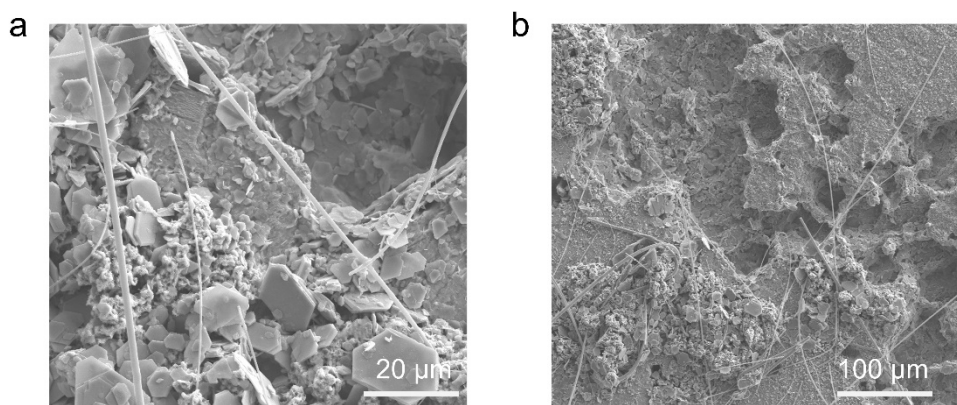


Fig. S6. SEM images of the Zn anodes after 50 cycles at 5 mA cm⁻², 5 mA h cm⁻² in ZS electrolyte.

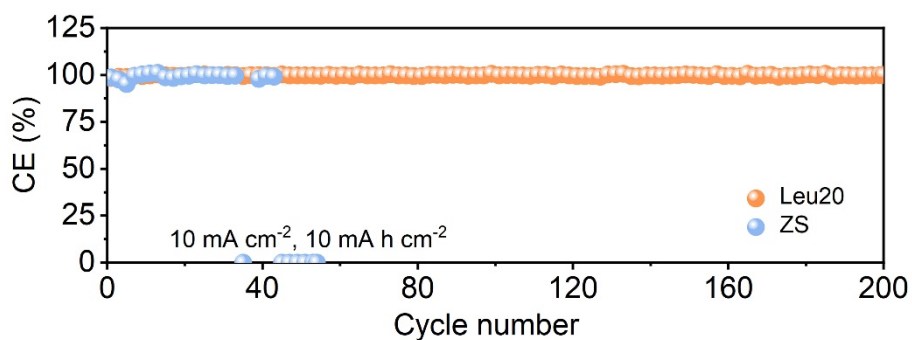


Fig. S7. CE performance of Zn||Cu asymmetric cells assembled with Leu20 and ZS electrolyte at 10 mA cm⁻², 10 mA h cm⁻².

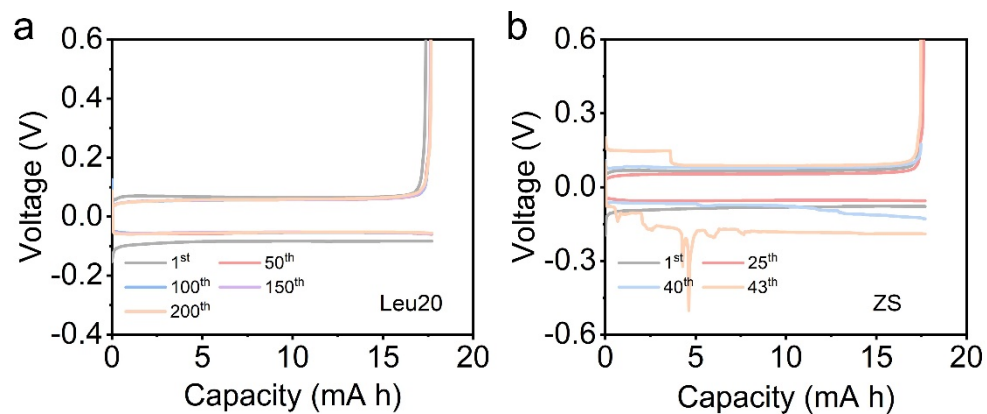


Fig. S8. Voltage profiles of Zn||Cu asymmetric cells based on (a) Leu20 and (b) ZS electrolytes at 10 mA cm^{-2} , 10 mA h cm^{-2} .

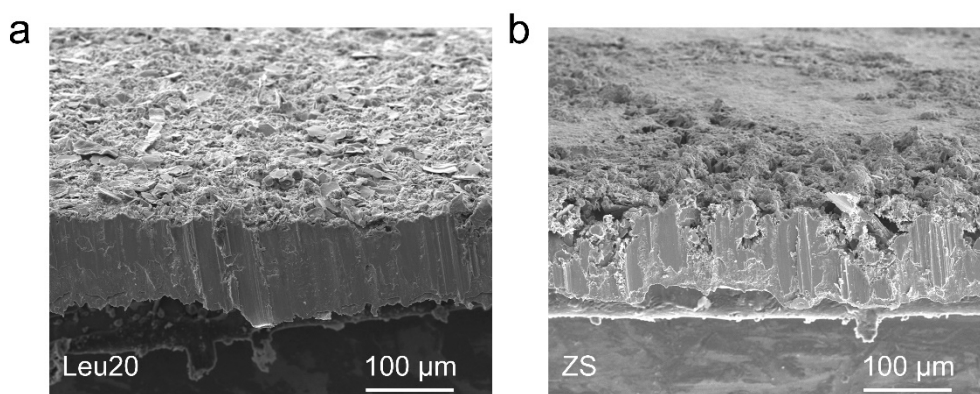


Fig. S9. Cross-sectional SEM images of the Zn anodes after 25 cycles at 1 mA cm^{-2} , 1 mA h cm^{-2} in (a) Leu20 and (b) ZS electrolytes.

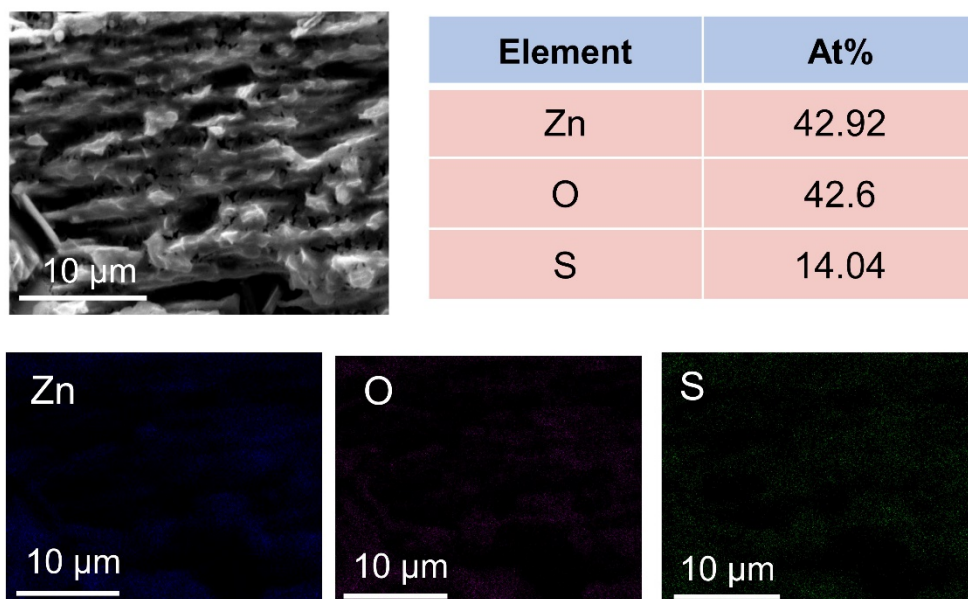


Fig. S10. EDS spectrum and elemental mappings on the Zn anode surface after cycling in Leu20 electrolyte at 10 mA cm^{-2} , 10 mA h cm^{-2} .

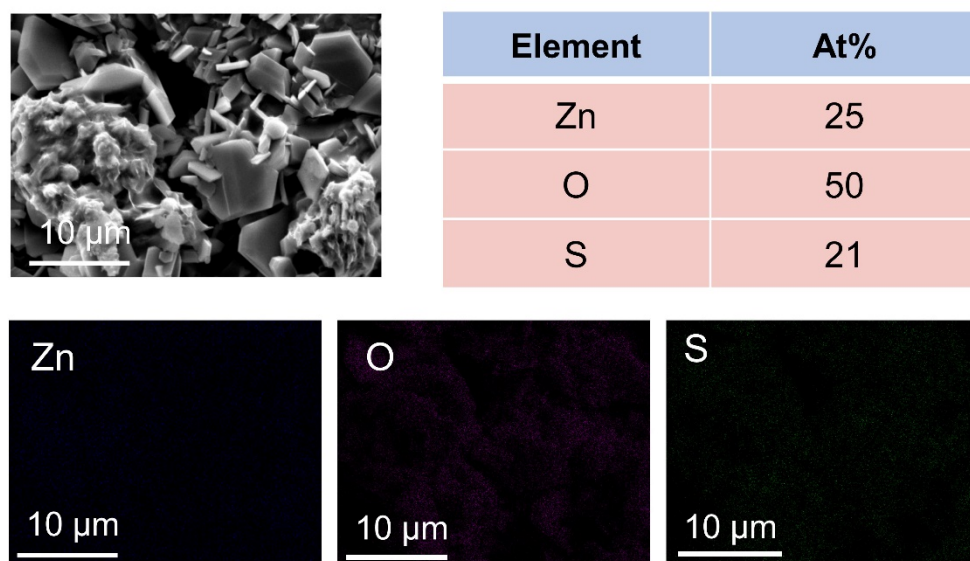


Fig. S11. EDS spectrum and elemental mappings on the Zn anode surface after cycling in ZS electrolyte at 10 mA cm^{-2} , 10 mA h cm^{-2} .

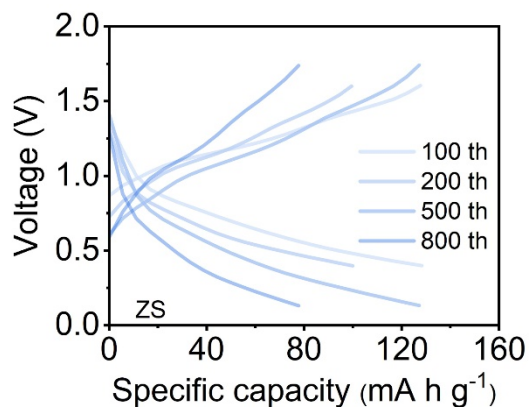


Fig. S12. Voltage profiles of Zn||NH₄V₄O₁₀ full cell assembled with ZS electrolyte at a current density of 2 A g⁻¹.

References

- 1 D. W. Christopher, C. Paola, J. Chem. Phys, 2015, **143**, 174502.
- 2 "The Sobtop software", can be found under <http://sobereva.com/soft/Sobtop> (accessed 2 March 2024), uploaded 17 February 2024 by T. Lu.
- 3 T. Lu, F. Chen, J. Comput. Chem, 2012, **35**, 580-592.
- 4 W. Humphrey, A. Dalke, K. Schulten, J. Mol. Graph. Model, 1996, **14**, 33-38.